

Critical adsorption on non-spherical colloidal particles

S. Kondrat, L. Harnau, and S. Dietrich

*Max-Planck-Institut für Metallforschung, Heisenbergstr. 3, D-70569 Stuttgart, Germany,
and Institut für Theoretische und Angewandte Physik,
Universität Stuttgart, Pfaffenwaldring 57, D-70569 Stuttgart, Germany*

(Dated: October 27, 2018)

We consider a non-spherical colloidal particle immersed in a fluid close to its critical point. The temperature dependence of the corresponding order parameter profile is calculated explicitly. We perform a systematic expansion of the order parameter profile in powers of the local curvatures of the surface of the colloidal particle. This curvature expansion reduces to the short distance expansion of the order parameter profile in the case that the solvent is at the critical composition.

PACS numbers: 64.60.Fr, 68.35.Rh, 82.70.Dd, 64.75.+g

I. INTRODUCTION

Various interactions between colloidal particles immersed in a solvent can influence the properties of the system. In a colloidal suspension containing particles of different size, there is an effective attractive interaction between larger particles. This attraction is due to the extra volume that becomes available to smaller particles when larger particles approach each other, leading to an overlap of excluded volumes which increases the entropy of the system (see, e.g., Ref. [1] and references therein). Colloidal particles, surfaces of which dissociate in solution, exhibit a screened Coulomb interaction due to charged surfaces of the particles and the surrounding counterions (see, e.g., Ref. [2]). Van der Waals dispersion forces arise from induced dipole-dipole interactions due to quantum mechanical fluctuations of the charge density (see, e.g., Ref. [3]). The confinement of critical order parameter fluctuations in a binary liquid mixture near its critical demixing point give rise to long-ranged critical Casimir forces between immersed colloidal particles (see, e.g., Ref. [4]). The richness of the physical properties of colloidal suspensions is mainly based on the possibility to tune these interactions which differ significantly in strength and range. In the case of the effective entropic interaction, the Coulomb interaction, and the van der Waals interaction this tuning is accomplished by changing the composition of the solvent by adding depletion agents, salt, or other components. For example, by matching the indices of refraction of the colloidal particles and the solvent it is possible to effectively switch off the dispersion forces and to create colloidal suspensions in which the actual effective interaction between uncharged colloidal particles very closely resembles a hard core potential. In the case of charged colloidal particles, even small polyelectrolyte additives can have substantial impact on the aggregation and kinetic stability of the charged particles [5]. Compared with such modifications, changes of the temperature or pressure typically result only in minor changes of the effective interaction between colloidal particles. However, effective interactions generated by bringing solvents close to a phase transition of their own are ex-

tremely sensitive to such changes as observed experimentally [6, 7, 8, 9, 10, 11, 12, 13, 14, 15, 16]. In these experiments, a dilute suspension of spherical colloidal particles has been formed within the one-phase region of a binary liquid mixture acting as the solvent. As the temperature of the system approaches the phase separation temperature of the binary liquid mixture, the colloidal particles aggregate and flocculate out of solution. Light scattering measurements indicate that an adsorption layer rich in one of the two solvent species forms around each colloidal particle. The experimental results strongly suggest that the colloidal aggregation behavior is induced by the presence of this adsorption layer. The thickness of the layer increases upon approaching the aggregation line in the phase diagram.

In a classical binary liquid mixture near its critical demixing point, the order parameter is a suitable concentration difference between the two species forming the liquid. The generic preference of confining boundaries for one of the two species results in the presence of effective surface fields leading to nonvanishing order parameter profiles even in the one-phase region of the phase diagram [17, 18]. These critical adsorption profiles become particularly long-ranged due to correlation effects induced by the critical fluctuations of the order parameter of the solvent. While several theoretical investigations have been devoted to the understanding of critical adsorption phenomena on planar walls and spherical particles (see Refs. [4, 19] and references therein), critical adsorption on non-spherical particles has been studied only in the limiting cases of infinitely long cylinders [20] and very small dumbbells and ellipsoids within the framework of a small particle operator expansion [21], despite the growing interest in non-spherical colloidal particles (see, e.g., Refs. [1, 22]). Due to the reduced symmetry of the shapes of non-spherical colloidal particles compared with spherical symmetry the interactions between them depend not only on the separation between their centers but also on their mutual orientations. As a result various properties of fluids consisting of such particles differ from the corresponding ones of fluids consisting of spherical particles. As a prerequisite for studies – motivated by the aforementioned aggregation phenomena

near criticality – on critical Casimir forces between non-spherical colloidal particles and surfaces we investigate here systematically the temperature dependence of critical adsorption on a single colloidal particle. In order to treat ellipsoids, spheres, and cylinders in a unified way within the appropriate field-theoretical approach and for general embedding dimensions D it is helpful to consider the particle shape of a hypercylinder defined as

$$\mathcal{K}_d(\{R_i\}) = \left\{ \mathbf{r} = (x_1, x_2, \dots, x_D) \right. \\ \left. \left| \sum_{s=1}^d \left(\frac{x_s}{R_s} \right)^2 \leq 1, \quad d \leq D \right. \right\}, \quad (1)$$

where $R_1 \leq R_2 \leq \dots \leq R_d$ are the semi-axes of the particle (see Fig. 1). In the case of equal semi-axes $R_1 = R_2 = \dots = R_d$ the hypercylinder reduces to the so called generalized cylinder with an infinitely extended "axis" of dimension $D - d$ [20, 23]. In $D = 3$ the "axis" can be the axis of an ordinary infinitely elongated cylinder ($d = 2$), or the midplane of slab ($d = 1$), or the center of a sphere ($d = 3$). In the case that not all semi-axes are equal but $d = D$ the hypercylinder reduces to an ellipsoid which is called a spheroid if the lengths of two semi-axes are the same. In $D = 3$ one may distinguish prolate spheroids ($R_1 = R_2 < R_3$) from oblate spheroids ($R_1 < R_2 = R_3$). The general ellipsoid ($R_1 < R_2 < R_3$) is called a triaxial ellipsoid. The generalization of D to values different from three is introduced for technical reasons because $D_{uc} = 4$ is the upper critical dimension for the relevance of fluctuations of the order parameter leading to a behavior different from that obtained from mean field theory valid in $D = 4$. It proves convenient to express the position vector \mathbf{r} in terms of a distance r_\perp perpendicular to the surface and dimensionless angles $\{\theta_s\}$, $s = 2, \dots, D$ (see Fig. 1). Moreover, the shape of a hypercylinder can be characterized by the smallest semi-axis $R \equiv R_1$ and the dimensionless ratios $\{\delta_s = R_s/R\}$, $s = 2, \dots, d$.

II. ORDER PARAMETER PROFILES

A. Scaling properties and short distance expansion

Close to T_c the critical adsorption on the surface of the mesoscopic particle is characterized by an order parameter profile $\langle \phi(\mathbf{r}) \rangle_t$ which takes the following scaling form

$$\langle \phi(\mathbf{r}) \rangle_t = a|t|^\beta P_\pm(r_\perp/\xi_\pm, R/\xi_\pm, \{\theta_s\}, \{\delta_s\}) \quad (2)$$

for distances r_\perp from the surface sufficiently larger than a typical microscopic length. Here $\langle \dots \rangle_t$ denotes the thermal average. $\xi_\pm(t \rightarrow 0) = \xi_0^\pm |t|^{-\nu}$ is the bulk correlation length above (+) or below (-) the critical temperature T_c , where $t = (T - T_c)/T_c$ is the reduced temperature and

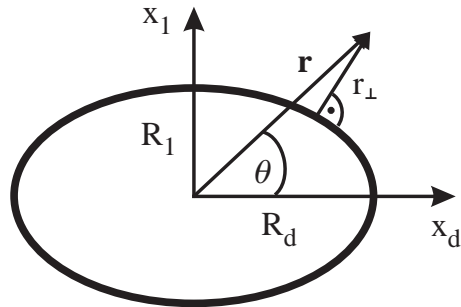


FIG. 1: Schematic side view of an ellipsoid with semi-axes $R \equiv R_1 \leq R_2 \leq \dots \leq R_d$. Only the projection of the particle onto the $x_1 - x_d$ plane is shown. Any point \mathbf{r} outside the particle can be reached by a distance r_\perp measured from the point closest to \mathbf{r} on the surface of the particle. The angle between the position vector of the latter surface point and the x_d axis is denoted as $\theta \equiv \theta_d$.

β and ν are the standard bulk critical exponents. The scaling functions $P_\pm(r_\perp/\xi_\pm, R/\xi_\pm, \{\theta_s\}, \{\delta_s\})$ are universal once the nonuniversal bulk amplitudes a and ξ_0^\pm are fixed by the value $\langle \phi_b \rangle_{t \rightarrow 0^-} = a|t|^\beta$ of the order parameter in the unbounded bulk and by the true correlation length defined by the exponential decay of the bulk two-point correlation function in real space. Therefore one finds $P_-(r_\perp/\xi_- \rightarrow \infty, R/\xi_-, \{\theta_s\}, \{\delta_s\}) = 1$ and $P_+(r_\perp/\xi_+ \rightarrow \infty, R/\xi_+, \{\theta_s\}, \{\delta_s\}) = 0$. In the opposite limit $r_\perp/\xi_\pm \rightarrow 0$, i.e., $T \rightarrow T_c$, the scaling functions and the order parameter profile exhibit short-distance singularities in the form of power laws which reflect the anomalous scaling dimension of the order parameter:

$$\langle \phi(\mathbf{r}) \rangle_{t=0} = aC_\pm(r_\perp/R, \{\theta_s\}, \{\delta_s\}) \left(\frac{r_\perp}{\xi_0^\pm} \right)^{-\beta/\nu}. \quad (3)$$

The ratio β/ν of the critical exponents has the value 1 in $D = 4$, ≈ 0.517 in $D = 3$ [24], and $1/8$ in $D = 2$. The amplitude functions $C_\pm(r_\perp/R, \{\theta_s\}, \{\delta_s\})$ are universal but depend on the definition of the correlation length, as the scaling functions $P_\pm(r_\perp/\xi_\pm, R/\xi_\pm, \{\theta_s\}, \{\delta_s\})$, too. Using the operator-product expansion (see, e.g., Refs. [25, 26]) a short distance expansion of the universal amplitude functions can be derived:

$$\frac{C_\pm(r_\perp/R \rightarrow 0, \{\theta_s\}, \{\delta_s\})}{c_\pm} = 1 + \lambda_H H \frac{r_\perp}{R} \\ + [\lambda_K K + \lambda_{H^2} H^2] \left(\frac{r_\perp}{R} \right)^2 \\ + [\lambda_{H^3} H^3 + \lambda_{HK} HK + \lambda_{G^2} G^2] \left(\frac{r_\perp}{R} \right)^3 + O\left(\frac{r_\perp}{R} \right)^4, \quad (4)$$

where $H \equiv H(\{\theta_s\}, \{\delta_s\})$, $K \equiv K(\{\theta_s\}, \{\delta_s\})$, and $G \equiv G(\{\theta_s\}, \{\delta_s\})$ are dimensionless local curvatures characterizing the surface and λ_I with $I = H, K, H^2, H^3, HK, G$ are dimensionless coefficients

which depend on D but not on the shape of the boundary surface, i.e., they are independent of $\{\theta_s\}$ and $\{\delta_s\}$. The dimensionless local curvatures are related to the local radii of curvature $A_i \equiv A_i(\{\theta_s\}, \{\delta_s\})$ according to (see, e.g., Ref. [28])

$$H = R \sum_{i=1}^{D-1} A_i^{-1}, \quad K = R^2 \sum_{\substack{i,j=1 \\ i < j}}^{D-1} A_i^{-1} A_j^{-1}, \quad (5a)$$

$$G = R^3 \sum_{\substack{i,j,k=1 \\ i < j < k}}^{D-1} A_i^{-1} A_j^{-1} A_k^{-1}. \quad (5b)$$

In the limit $r_\perp/R \rightarrow 0$ the universal amplitude functions $C_\pm(r_\perp/R = 0, \{\theta_s\}, \{\delta_s\})$ reduce to the universal amplitudes c_\pm for the critical adsorption profiles near planar walls confining semi-infinite systems [27]. According to Eq. (3) $C_-(r_\perp/R, \{\theta_s\}, \{\delta_s\}) = (\xi_0^+/\xi_0^-)^{\beta/\nu} C_+(r_\perp/R, \{\theta_s\}, \{\delta_s\})$, where $(\xi_0^+/\xi_0^-)^{\beta/\nu} = c_-/c_+ \approx 1.4$ (for $D = 3$) is a universal amplitude ratio which depends on the embedding dimension D (see Table I in Ref. [20]). Therefore it is sufficient to consider only one of these functions.

In the case of a sphere, i.e., $H^{(sph)} = D - 1$, $K^{(sph)} = (D - 1)(D - 2)/2$, and $G^{(sph)} = (D - 1)(D - 2)(D - 3)/6$, the universal amplitude functions are known exactly for any spatial dimension D by means of a finite conformal mapping from the half-space [29]:

$$C_+^{(sph)}(r_\perp/R) = c_+ \left(1 + \frac{1}{2} \frac{r_\perp}{R}\right)^{-\beta/\nu}. \quad (6)$$

A comparison of the short distance expansion of $C_+^{(sph)}(r_\perp/R)$ with Eq. (4) yields

$$\lambda_H(D - 1) = -\frac{1}{2} \frac{\beta}{\nu} \quad (7)$$

and [20]

$$(D - 1) \left(\frac{\lambda_K(D - 2)}{2} + \lambda_{H^2}(D - 1) \right) = \frac{1}{8} \frac{\beta}{\nu} \left(\frac{\beta}{\nu} + 1 \right), \quad (8)$$

as well as

$$(D - 1) \left(\lambda_{H^3}(D - 1)^2 + \frac{\lambda_{HK}(D - 1)(D - 2)}{2} + \frac{\lambda_G(D - 2)(D - 3)}{6} \right) = -\frac{1}{48} \frac{\beta}{\nu} \left(2 + 3 \frac{\beta}{\nu} + \frac{\beta^2}{\nu^2} \right). \quad (9)$$

In $D = 2$ all coefficients λ_I with $I = H, H^2, H^3$ can be deduced from Eqs. (7) - (9). For $D > 2$ a determination of the coefficients appearing in Eqs. (8) and (9) would require the additional knowledge of universal amplitude functions around differently shaped walls. However, these functions are not available beyond the mean field approach discussed in Sec. III below.

B. Curvature expansion

Recently a curvature expansion of the density profile of a hard sphere fluid close to a big convex particle has been proposed and successfully applied to the density profile around a hard ellipsoid [30]. The curvature expansion separates the properties of the fluid from the geometry of the big particle and allows one to determine density profiles in complex geometries based on those obtained in much simpler geometric configurations. Assuming that an analogous curvature expansion holds for the order parameter profile $\langle \phi(\mathbf{r}) \rangle_t$ leads to

$$\begin{aligned} \langle \phi(\mathbf{r}) \rangle_t &= \phi_t^{(p)}(r_\perp) + \phi_t^{(H)}(r_\perp, R)H \\ &+ \phi_t^{(K)}(r_\perp, R)K \phi_t^{(H^2)}(r_\perp, R)H^2 + \phi_t^{(H^3)}(r_\perp, R)H^3 \\ &+ \phi_t^{(HK)}(r_\perp, R)HK + \phi_t^{(G)}(r_\perp, R)G + O(R^{-4}), \quad (10) \end{aligned}$$

where $\phi_t^{(p)}(r_\perp)$ is the order parameter profile for the half-space bounded by a planar wall and $\phi_t^{(I)}(r_\perp, R)$ with $I = H, K, H^2, HK, H^3, G$ are expansion coefficient functions. A comparison of this equation with Eqs. (3) and (4) leads to the following short distance behavior of the curvature expansion coefficient functions:

$$\begin{aligned} \phi_t^{(p)}(r_\perp) &= ac_\pm \left(\frac{r_\perp}{\xi_0^\pm} \right)^{-\beta/\nu} \psi_\pm^{(p)}(r_\perp/\xi_\pm), \\ \psi_\pm^{(p)}(0) &= 1, \quad (11) \end{aligned}$$

$$\begin{aligned} \phi_t^{(I)}(r_\perp, R) &= ac_\pm \left(\frac{r_\perp}{\xi_0^\pm} \right)^{-\beta/\nu} \left(\frac{r_\perp}{R} \right)^n \lambda_I \psi_\pm^{(I)}(r_\perp/\xi_\pm), \\ \psi_\pm^{(I)}(0) &= 1, \quad (12) \end{aligned}$$

where $n = 1$ for $I = H$, $n = 2$ for $I = K$ and $I = H^2$, $n = 3$ for $I = HK$ and $I = H^3$ as well as $I = G$. These equations demonstrate the link between the short distance expansion of the universal amplitude function [Eq. (4)] and the curvature expansion of the order parameter profile [Eq. (10)]. The temperature dependence of the short distance expansion coefficient functions $\psi_\pm^{(I)}(r_\perp/\xi_\pm)$ follows from simple scaling considerations of the order parameter [31, 32] applied to the system under consideration:

$$\begin{aligned} \psi_\pm^{(I)}(r_\perp/\xi_\pm \rightarrow 0) &= 1 + \psi_{1,\pm}^{(I)} \left(\frac{r_\perp}{\xi_\pm} \right)^{1/\nu} \\ &+ \psi_{2,\pm}^{(I)} \left(\frac{r_\perp}{\xi_\pm} \right)^{2/\nu} + \psi_{D,\pm}^{(I)} \left(\frac{r_\perp}{\xi_\pm} \right)^D + \dots \\ &= 1 + \psi_{1,\pm}^{(I)} \left(\frac{r_\perp}{\xi_0^\pm} \right)^{1/\nu} |t| + \psi_{2,\pm}^{(I)} \left(\frac{r_\perp}{\xi_0^\pm} \right)^{2/\nu} t^2 \\ &+ \psi_{D,\pm}^{(I)} \left(\frac{r_\perp}{\xi_0^\pm} \right)^D |t|^{D\nu} + \dots \quad (13) \end{aligned}$$

where $I = p, H, K, H^2, HK, H^3, G$. Since the last term in Eq. (13) represents the leading non-analytic contribution to the order parameter profile for $t \rightarrow 0$, one

has $\psi_{1,-}^{(I)}(\xi_0^+)^{1/\nu} = -\psi_{1,+}^{(I)}(\xi_0^-)^{1/\nu}$ and $\psi_{2,-}^{(I)}(\xi_0^+)^{2/\nu} = \psi_{2,+}^{(I)}(\xi_0^-)^{2/\nu}$.

III. MEAN FIELD THEORY

Within a field theoretical renormalization group approach the scaling functions introduced above can be determined in lowest order perturbation theory within the framework of mean field theory corresponding to $\epsilon = 4 - D = 0$. A renormalization group enhanced mean field theory is obtained by using for the scaling variables entering into scaling functions their full scaling form for $\epsilon = 1$. The standard Ginzburg-Landau fixed-point Hamiltonian for describing critical phenomena is given by [33, 34]

$$\mathcal{H}[\phi] = \int_V dV \left(\frac{1}{2}(\nabla\phi)^2 + \frac{\tau}{2}\phi^2 + \frac{u}{24}\phi^4 \right). \quad (14)$$

This Hamiltonian has to be supplemented by the boundary condition $\phi = +\infty$ at the surface of the colloidal particle corresponding to the critical adsorption fixed point [35]. The integration runs over the volume accessible to the fluid and the parameter τ is proportional to the reduced temperature t . Within mean field theory $\tau = t/(\xi_0^+)^2$ for $T > T_c$ and $\tau = -|t|/(\xi_0^-)^2/2$ for $T < T_c$ with $\xi_0^+/\xi_0^- = \sqrt{2}$. The coupling constant $u > 0$ stabilizes the Hamiltonian $\mathcal{H}[\phi]$ for temperatures below the critical point ($T < T_c$) and $(\nabla\phi)^2$ penalizes spatial variations of the order parameter. Within mean field theory fluctuations of the order parameter are neglected and only the configuration of the order parameter with the largest statistical weight $m = \sqrt{u/6}\langle\phi\rangle$ with $\sqrt{u/6} = \sqrt{|\tau|/|t|}/a$ is taken into account. After functional minimization one obtains the Euler-Lagrange equation

$$\Delta m = \tau m + m^3. \quad (15)$$

Equation (15) can be solved numerically for arbitrary temperatures. For computational purposes it is convenient to choose a spheroidal coordinate system in which the surface of the ellipsoid corresponds to a constant value of one spheroidal coordinate (see, e.g., Ref. [36]). In the case of a generalized cylinder the Euler-Lagrange equation reduces to [20]

$$\frac{\partial^2}{\partial r_\perp^2} m(r_\perp, R, \tau) + \frac{d-1}{r_\perp + R} \frac{\partial}{\partial r_\perp} m(r_\perp, R, \tau) = \tau m(r_\perp, R, \tau) + m^3(r_\perp, R, \tau), \quad (16)$$

where $d = 1, 2, 3, 4$ denotes different types of generalized cylinders. Using the short distance expansion [Eq. (4)] for the universal amplitude function $C_+(r_\perp/R) = r_\perp m(r_\perp, R, \tau = 0)$ [Eq. (3)] as input into Eq. (16) and equating terms of the same power in r_\perp/R

leads to

$$\begin{aligned} \lambda_H &= -\frac{1}{6}, & \lambda_K &= -\frac{1}{3}, & \lambda_{H^2} &= \frac{5}{36}, \\ \lambda_{H^3} &= -\frac{31}{216}, & \lambda_{HK} &= \frac{1}{2}, & \lambda_G &= -\frac{3}{4}, \end{aligned} \quad (17)$$

where $H = d - 1$, $K = (d - 1)(d - 2)/2$, and $G = (d - 1)(d - 2)(d - 3)/6$.

A. Curvature expansion coefficient functions

The curvature expansion coefficient functions in Eq. (10) are determined by solving Eq. (16) for the four generalized cylinders with high symmetries and for arbitrary values of τ . In the following we restrict our presentation to the case $T > T_c$. The first curvature expansion coefficient function is known analytically [20] (see also the Appendix):

$$\psi_+^{(p)}(\zeta_+ = r_\perp/\xi_+) = \frac{\zeta_+}{\sinh(\zeta_+)}. \quad (18)$$

Our numerical data obtained from Eq. (16) for $d = 2, 3, 4$ can be used to determine individually all coefficient functions appearing in Eq. (10). Moreover, the internal consistency of Eq. (10) can be checked in the case of the functions $\phi_t^{(H)}(r_\perp, R)$, $\phi_t^{(K)}(r_\perp, R)$, and $\phi_t^{(H^2)}(r_\perp, R)$ in addition to the function $\phi_t^{(p)}(r_\perp)$ for the half-space. This means that first each of these functions is determined separately for each value of d , e.g., $\phi_{t,d=2}^{(H)}(r_\perp, R)$, $\phi_{t,d=3}^{(H)}(r_\perp, R)$, and $\phi_{t,d=4}^{(H)}(r_\perp, R)$. Thereafter these three functions as obtained this way are compared with each other. Internal consistency means that these three functions are identical within the numerical accuracy. For higher orders $n \geq 3$ in Eq. (12), there are contributions of more than two coefficient functions to the curvature expansion. A consistency check for these functions would require the additional knowledge of the order parameter profiles around differently shaped surfaces. For comparison we note that in the case of the aforementioned curvature expansion of density profiles of a hard sphere fluid around an ellipsoid in $D = 3$ it was possible to check the internal consistency of the curvature expansion only in the case of the density profiles corresponding to $\phi_t^{(H)}(r_\perp, R)$ and $\phi_t^{(p)}(r_\perp)$ [30]. Hence the present calculation in $D = 4$ provides a more stringent consistency test. Figures 2 (a) and (b) display the curvature expansion coefficient functions except for the well-known function $\psi_+^{(p)}(\zeta_+ = r_\perp/\xi_+)$ for the half-space [Eq. (18)]. One observes that all coefficient functions attain the contact value 1 at $\zeta_+ = 0$ due to $\psi_+^{(I)}(\zeta_+ \rightarrow 0) - 1 = a_+^{(I)}(\zeta_+)^{1/\nu}$ in agreement with Eq. (13), where $\nu = 1/2$ within mean field theory and $a_+^{(I)}$ is a dimensionless coefficient (see the Appendix). Moreover, all coefficient functions exhibit an exponential decay for large values of the scaling variable $\zeta_+ = r_\perp/\xi_+$. We have verified numerically the internal

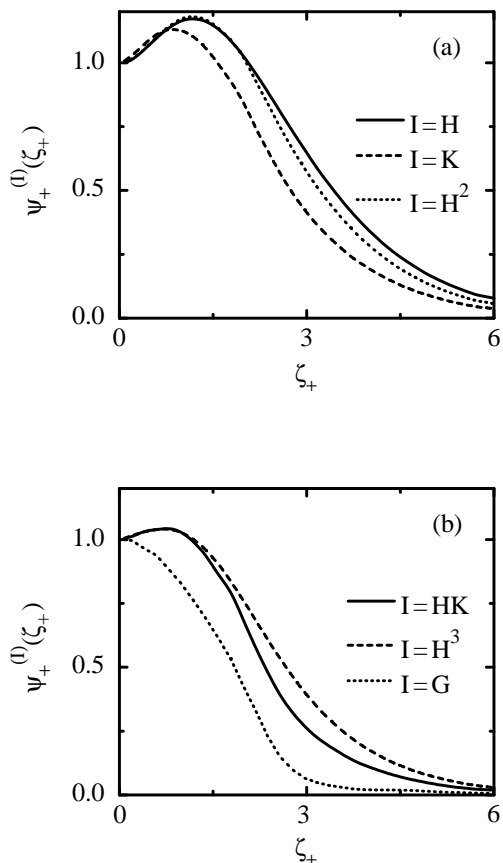


FIG. 2: (a) [(b)] The curvature expansion coefficient functions $\psi_+^{(1)}(\zeta_+ = r_\perp/\xi_+)$ for $I = H, K, H^2$ [HK, H^3, G] of the order parameter profile for critical adsorption on curved surfaces according to Eqs. (12) and (13). The coefficient functions have been determined from the numerical solution of Eq. (16) for $d = 2, 3, 4$ corresponding to three different types of generalized cylinders with high symmetries in spatial dimension $D = 4$. All coefficient functions attain the finite value 1 as $\zeta_+ \rightarrow 0$ (see Eq. (13)).

consistency of the first four terms of the curvature expansion [Eq. (10)] as discussed above.

B. Scaling functions

We now turn our attention to the order parameter profiles around the ellipsoidal particle shown in Fig. 1. In Figs. 3 (a) and (b) the scaling function $P_+ = |\tau|^{-1/2}m(\tau)$ of the order parameter profile is shown for two angles θ as obtained from Eq. (15) together with the results of the curvature expansion [Eq. (10)]. For $\theta = \pi/2$ and $R/\xi_+ = 30$ (lower curves in Fig. 3 (a)) the results obtained from the curvature expansion are in agreement basically everywhere with the direct calculations of the scaling function. With increasing local curvatures (see Fig. 1), i.e., for $\theta = 0$ and $R/\xi_+ = 30$ in Fig. 3 (a) (upper curves) as well as for $\theta = 0, \pi/2$ and

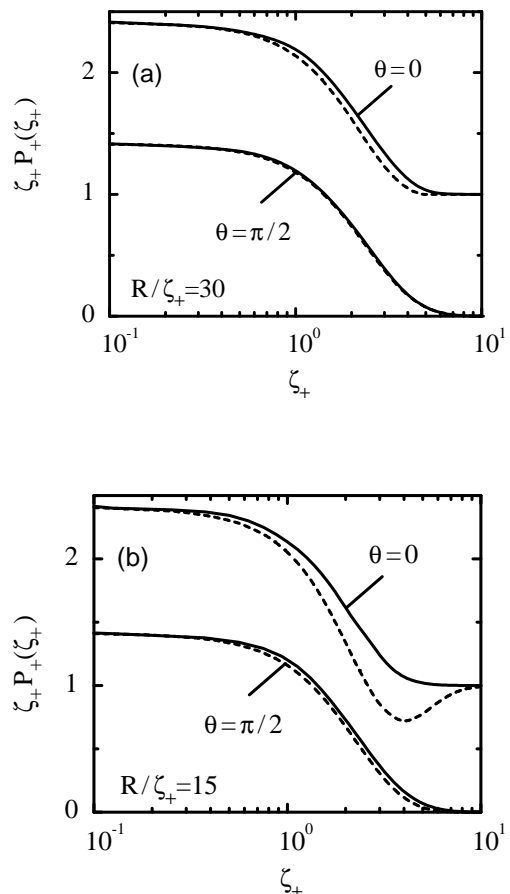


FIG. 3: (a) [(b)] The scaling function $P_+(\zeta_+ = r_\perp/\xi_+, R/\xi_+, \{\theta_s\}, \{\delta_s = R_s/R\})$ [Eq. (2)] of the order parameter profile for critical adsorption on an ellipsoid (see Fig. 1) with $R/\xi_+ = 30$ [$R/\xi_+ = 15$] and $\delta_2 = \delta_3 = \delta_4/2 = 1$ in dimension $D = 4$ for the angles $\theta = \theta_4 = \pi/2$ (lower curves) and $\theta = \theta_4 = 0$ (upper curves). For symmetry reasons the order parameter profile is independent of the angles θ_2 and θ_3 . Direct numerical calculations (solid lines) according to Eq. (15) are compared with the curvature expansion up to and including third order (dashed lines) as obtained from Eq. (10). The upper two curves have been shifted up by 1.

$R/\xi_+ = 15$ in Fig. 3 (b), the third-order curvature expansion (i.e., including terms up to $n \leq 3$) and the direct calculations deviate from each other for scaled distances $\zeta_+ = r_\perp/\xi_+ \gtrsim H, K, G$ because higher order terms in the curvature expansion are required. Nevertheless, the calculations support the use of the curvature expansion of the order parameter profile as a first approximation for large ellipsoids.

The scaling function of the order parameter profile for an ellipsoid with two equal small ($R = R_1 = R_2$) and two equal large semi-axes ($R_3 = R_4$) is shown in Fig. 4. In the limit of a large aspect ratio $R_4 \gg R$ of the ellipsoid the scaling function reduces to the one for a generalized cylinder with $d = 2$ in Eq. (16). In the case that all semi-axes are the same the result for a sphere

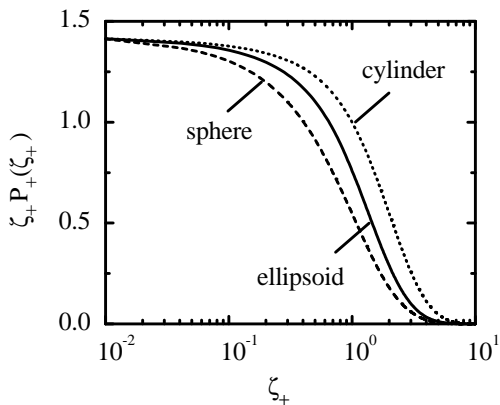


FIG. 4: The scaling function $P_+(\zeta_+ = r_\perp/\xi_+, R/\xi_+, \{\theta_s\}, \{\delta_s = R_s/R\})$ (solid line) of the order parameter profile for critical adsorption on an ellipsoid with $\delta_2 = \delta_3/2 = \delta_4/2 = 1$ and for the angles $\theta = \theta_4 = \pi/2$ (see Fig. 1) in dimension $D = 4$. For symmetry reasons the order parameter profile is independent of the angles θ_2 and θ_3 . The dashed and dotted lines represent the results for a sphere with equal semi-axes $\delta_2 = \delta_3 = \delta_4 = 1$ and a generalized cylinder with $\delta_2 = 1 \ll \delta_3 = \delta_4$ corresponding to $d = 4$ and $d = 2$ in Eq. (16), respectively. The smallest semi-axis is fixed to $R/\xi_+ = 0.6$ for the ellipsoid, the sphere, and the generalized cylinder.

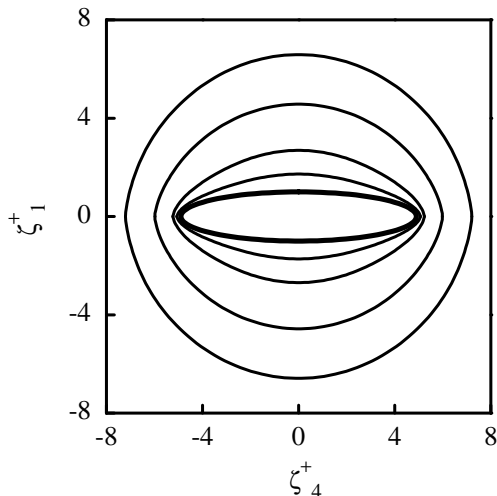


FIG. 5: The contour lines of the scaling function $P_+(\zeta_+ = r_\perp/\xi_+, R/\xi_+, \{\theta_s\}, \{\delta_s = R_s/R\})$ of the order parameter profile for critical adsorption on an ellipsoid (thick line) in $D = 4$ with $R/\xi_+ = 1$ and $\delta_2 = \delta_3 = \delta_4 = 5$. The center of the ellipsoid is located at the origin of the coordinate system and only the contour lines in the $\zeta_1^+ - \zeta_4^+$ plane are shown, where $\zeta_1^+ = x_1/\xi_+$ and $\zeta_4^+ = x_4/\xi_+$ (see Fig. 1). The curves correspond to the following values of P_+ : 4, 1, 0.1, 0.01 (from the middle to the outside).

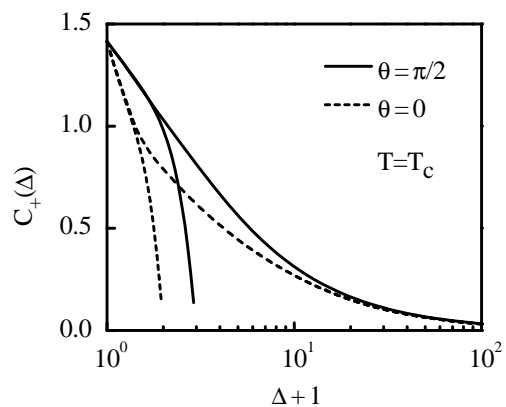


FIG. 6: The universal amplitude function $C_+(\Delta = r_\perp/R, \{\theta_s\}, \{\delta_s = R_s/R\})$ for an ellipsoid with $\delta_2 = \delta_3 = \delta_4/2 = 1$ within mean-field approximation (i.e., $D = 4$) for the angles $\theta = \theta_4 = \pi/2$ and $\theta = 0$ (see Fig. 1). For symmetry reasons the order parameter profile is independent of the angles θ_2 and θ_3 . The short lines show the results obtained from the short distance expansion (up to and including the order indicated in Eq. (4)). All curves share the common value $C_+(\Delta = 0, \{\theta_s\}, \{\delta_s = R_s/R\}) = c_+ = \sqrt{2}$ corresponding to the universal amplitude for the half-space.

is recovered. From Fig. 5 one can infer that the contour lines of the scaling function of the order parameter profile quickly exhibit spherical symmetry with increasing distance from the surface of an ellipsoid. Along the radial direction $\theta = 0$ (i.e., for $\zeta_1^+ = x_1/\xi_+ = 0$) the scaling function decays faster away from the surface than along the radial direction $\theta = \pi/2$ (i.e., for $\zeta_4^+ = x_4/\xi_+ = 0$) because the local curvatures H , K , and G of the surface at $\theta = 0$ are larger than at $\theta = \pi/2$ (see Fig. 1). For comparison we note that also in the case of generalized cylinders the decay rate of the scaling function increases upon increasing the local curvatures (see Figs. 5 and 6 in Ref. [20]).

C. Universal amplitude functions

Whereas the preceding subsection has been focused on adsorption phenomena on ellipsoidal particles for $T \neq T_c$, this subsection addresses the adsorption phenomena on ellipsoidal particles in the case that the suspending fluid is critical, i.e., at the critical composition and at $T = T_c$. The universal amplitude function $C_+(\Delta = r_\perp/R, \{\theta_s\}, \{\delta_s\})$ (see Eq. (3)) is shown in Figs. 6 and 7 for two different ellipsoids. According to Eq. (4) the function $C_+(\Delta, \{\theta_s\}, \{\delta_s\})$ starts at $C_+(\Delta = 0, \{\theta_s\}, \{\delta_s\}) = c_+$, where $c_+ = \sqrt{2}$ within mean field theory. Figure 6 shows the numerical results as obtained from Eq. (15) with $C_+ = r_\perp m(\tau = 0)$ together with the results according to the short distance expansion [Eq. (4)]. The calculations provide the range of validity $\Delta = r_\perp/R \lesssim H, K, G$ of the short distance

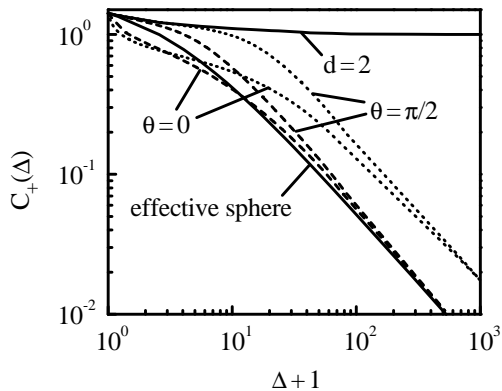


FIG. 7: The universal amplitude function $C_+(\Delta = r_\perp/R, \{\theta_s\}, \{\delta_s = R_s/R\})$ for two ellipsoids with two equal small and two equal large semi-axes $\delta_2 = \delta_3/25 = \delta_4/25 = 1$ (dotted lines) and $\delta_2 = \delta_3/4 = \delta_4/4 = 1$ (dashed lines) in mean-field approximation (i.e., $D = 4$). The upper [lower] dotted and dashed lines represent the results for the angle $\theta = \pi/2$ [$\theta = 0$] (see Fig. 1). For symmetry reasons the order parameter profile is independent of the angles θ_2 and θ_3 . The lower solid line represents the universal amplitude function for a sphere of radius $R_{eff} = R\sqrt{\delta_4^2 - 1}/\text{Arcosh}(\delta_4)$ with $\delta_4 = 4$ as obtained from Eq. (6). The upper solid line follows from Eq. (16) with $d = 2$ corresponding to a generalized cylinder with radius R and two infinitely extended axes, i.e., $\delta_2 = 1, \delta_3 = \delta_4 = \infty$. All curves share the common value $C_+(\Delta = 0, \{\theta_s\}, \{\delta_s = R_s/R\}) = \sqrt{2}$. For large distances from the surface the universal amplitude function vanishes as $\Delta^{-\beta/\nu}$ with $\beta/\nu = 1$ in the case of the sphere and the ellipsoids whereas for the generalized cylinder it tends to the finite value 1.

expansion. For comparison we note that the curvature expansion for $T \neq T_c$ provides a good approximation of the order parameter profile for all distances r_\perp from the surface provided the local curvatures are smaller than the correlation length (see Fig. 3). However, at the critical point the correlation length diverges and the curvature expansion, i.e., the short distance expansion, is valid only for distances from surface which are small compared with the local curvatures of the surface of the colloidal particle. Figure 7 demonstrates that the universal amplitude function decays proportional to $r_\perp^{-\beta/\nu}$ with $\beta/\nu = 1$ for large distance r_\perp from the surface. Far away from the surface of an ellipsoidal particle of arbitrary shape the universal amplitude function is angle-independent and given by $C_+^{(sph)}(r_\perp/R_{eff})$ [Eq. (6)] with an effective radius R_{eff} that depends on the aspect ratios δ_s of the ellipsoid (see the vanishing differences between the dashed lines and the lower solid line in Fig. 7 for large Δ). The expression $R_{eff} = R\sqrt{\delta_4^2 - 1}/\text{Arcosh}(\delta_4)$ for the effective radius follows from a small particle operator expansion, analogous to the one presented in Refs. [21, 37, 38], to the system under consideration in this limiting case characterized by semi-axes of the ellipsoids which are much smaller than other lengths such as the correlation length or the dis-

tance between the surface of the particle and the point at which the order parameter is monitored.

IV. SUMMARY

This work has been devoted to the investigation of critical adsorption phenomena on ellipsoidal colloidal particles [Fig. 1] which are immersed in a fluid near criticality, i.e., $t = (T - T_c)/T_c \rightarrow 0$ in the case that the fluid is at the critical composition. The adsorption profiles are characterized by universal scaling functions P_\pm for $T \neq T_c$ [Eq. (2)], involving the bulk correlations lengths ξ_\pm , and for $T = T_c$ by universal amplitude functions C_\pm [Eq. (3)].

For $T = T_c$ the short distance expansion of the universal amplitude function of the order parameter profile near a curved surface has been introduced [Eqs. (3) and (4)]. This expansion involves local curvatures of the surface [Eqs. (5a)]. Also for temperatures $T \neq T_c$ a curvature expansion of the order parameter has been considered [Eq. (10)] which involves the local curvatures of the surface, too. The short distance behavior of the latter curvature expansion coefficient functions [Eqs. (11) and (12)] is uniquely determined by a comparison of the curvature expansion [Eq. (10)] with the short distance expansion [Eq. (4)]. A numerical calculation within mean field theory [Eq. (14)] confirms this relation between the curvature expansion and the short distance expansion [Figs. 2 (a), (b) and 6].

For comparison we note that the contact values of curvature expansion coefficient functions of the density profile of a hard sphere fluid close to a hard convex wall are uniquely determined by exact statistical mechanical sum rules [39, 40] and the morphometric form of the grand potential [30, 41]. If motion invariance, continuity, and additivity of the grand potential are satisfied, only four morphometric measures are needed to describe fully the influence of an arbitrarily shaped wall on thermodynamic properties of fluids consisting of spherical and non-spherical [1] particles. Hadwiger's theorem [42, 43] states that every motion-invariant, continuous, and additive functional in three dimensions can be expressed in terms of a linear combination of only *four* integrated geometric properties: the volume, the surface area, the mean integrated curvature, and the Euler characteristic of the wall. Thermodynamically away from bulk and surface phase transitions and for short-ranged interactions and correlations between the fluid particles, it is therefore expected that the grand potential fulfills the requirements of Hadwiger's theorem. The value of the density profile at a confining hard surface can be regarded as a *thermodynamic* quantity because of exact sum rules implying that the values of the curvature expansion coefficient functions of the density profile *at a confining hard surface* can be expressed in terms of thermodynamic properties such as the pressure of the bulk fluid, the fluid - planar wall surface tension, and the bending rigidity. These ar-

guments are expected to be not applicable to critical phenomena because intrinsic lengths in such systems reach macroscopic sizes so that the assumption of additivity is no longer valid. This has been confirmed by an explicit calculation of the excess adsorption for a sphere and a cylinder immersed in a fluid near criticality (see Figs. 8 and 9 in Ref. [20]).

However, at T_c and *close to a confining surface* the curvature expansion coefficient functions of the order parameter profile for critical adsorption are determined by the short distance expansion of the universal amplitude functions as discussed above; this expansion involves arbitrarily high orders.

The curvature expansion for $T \neq T_c$ provides a reliable approximation of the order parameter profile for all distances from the surface provided the local curvatures are smaller than the inverse correlation length [Fig. 3], similar to the findings for the curvature expansion of the density profile of a hard sphere fluid close to a hard convex surface. However, at the critical point the correlation length diverges and the curvature expansion, which in this case reduces to the short distance expansion, is valid only for distances from surface which are small compared with the local radii of curvature of the surface of the colloidal particle [Fig. 6]. In this sense at T_c the curvature expansion breaks down as a globally reliable approximation.

The scaling functions for critical adsorption on ellipsoidal particles of various shapes and sizes have been determined numerically for $T \neq T_c$ within mean field theory [Figs. 3, 4, and 5]. In the case of very small or very large ratios of the semi-axes of the ellipsoid the results for a generalized cylinder such as a sphere or a rod are recovered. At the surface the explicit form of the universal amplitude function C_+ for an ellipsoid [Fig. 7] attains the value for the half-space and exhibits a power law limiting behavior far from the surface in accordance with the results for a sphere [Eq. (6)].

Acknowledgments

The authors thank R. Roth for useful discussions.

APPENDIX

In this appendix we briefly discuss how the coefficients $\psi_{1,\pm}^{(I)}, \psi_{2,\pm}^{(I)}, \dots$ for $I = p, H$ introduced in Eq. (13) can be calculated analytically within mean field theory, i.e., for $D = 4$. Since the approaches for $T > T_c$ and $T < T_c$ are similar we restrict our presentation to the case $T > T_c$ and drop the subscript '+' in order to simplify the notation.

In the case of a generalized cylinder the scaling function $P(\zeta = r_\perp/R, \alpha = R/\xi) = |\tau|^{-1/2} m(r_\perp, R, \tau)$ satis-

fies the Euler-Lagrange equation [Eq. (16)]

$$P''(\zeta, \alpha) + \frac{d-1}{\zeta+\alpha} P'(\zeta, \alpha) = P(\zeta, \alpha) + P^3(\zeta, \alpha), \quad (\text{A.1})$$

where the derivatives are taken with respect to the variable ζ . For $\alpha \gg 1$ one may assume that the scaling function is analytic in α^{-1} such that it can be expanded into a Taylor series around $\alpha^{-1} = 0$:

$$P(\zeta, \alpha \rightarrow \infty) = P_0(\zeta) + P_1(\zeta)\alpha^{-1} + \dots \quad (\text{A.2})$$

By using the expansion $(\zeta+\alpha)^{-1} = \alpha^{-1} + \dots$ in Eq. (A.1) in conjunction with Eq. (A.2) one obtains the familiar nonlinear differential equation for the profile near a planar wall confining a semi-infinite system,

$$P_0''(\zeta) = P_0(\zeta) + P_0^3(\zeta), \quad (\text{A.3})$$

with the solution

$$P_0(\zeta) = \frac{\sqrt{2}}{\sinh(\zeta)} = \frac{P_0^{(1)}}{\zeta} + P_0^{(2)}\zeta + P_0^{(3)}\zeta^3 + \dots \quad (\text{A.4})$$

and the linear differential equation

$$P_1''(\zeta) + (d-1)P_1'(\zeta) = P_1(\zeta) + 3P_0^2(\zeta)P_1(\zeta). \quad (\text{A.5})$$

While the profile $P_0(\zeta)$ is well-known we now turn our attention to the calculation of $P_1(\zeta)$. To this end we expand $P_1(\zeta)$ as

$$P_1(\zeta) = P_1^{(0)} + P_1^{(1)}\zeta + P_1^{(2)}\zeta^2 + P_1^{(3)}\zeta^3 + P_1^{(4)}\zeta^4 + \dots \quad (\text{A.6})$$

By inserting Eqs. (A.4) and (A.6) into Eq. (A.5) and equating terms with the same power in ζ one derives the coefficients

$$\begin{aligned} P_1^{(0)} &= -\frac{d-1}{3\sqrt{2}}, & P_1^{(1)} &= 0, \\ P_1^{(2)} &= -\frac{d-1}{6\sqrt{2}}, & P_1^{(4)} &= -\frac{d-1}{72\sqrt{2}}. \end{aligned} \quad (\text{A.7})$$

However, the value of $P_1^{(3)}$ cannot be determined this way, i.e., for *any* value of $P_1^{(3)}$ Eq. (A.5) is satisfied because of the *known* values of $P_0^{(1)}, P_0^{(2)}, P_0^{(3)}, \dots$. In Ref. [20] the following analytic solution of Eq. (A.5) has been proposed:

$$\begin{aligned} P_1(\zeta) &= (d-1) \frac{\cosh(\zeta) - \sinh(\zeta)}{6\sqrt{2} \sinh^2(\zeta)} \left[2 \cosh(2\zeta) - 2 - 3\zeta \right. \\ &\quad \left. - 3\zeta \cosh(2\zeta) + 3 \sinh(2\zeta) - 3\zeta \sinh(2\zeta) \right]. \end{aligned} \quad (\text{A.8})$$

This function can be expanded leading to the coefficients given in Eq. (A.7) and to

$$P_1^{(3)} = \frac{\sqrt{2}(d-1)}{15}. \quad (\text{A.9})$$

By inserting the scaling function $P(\zeta, \alpha)$ from Eqs. (A.2), (A.6), and (A.7) into Eq. (2) one obtains the expansion coefficient functions $\psi_1^{(I)}, \psi_2^{(I)}, \dots$ for $I = H$ in Eq. (13). We emphasize that a non-vanishing value of $P_1^{(3)}$ would lead to an additional *non-analytic* term $\sim t^{3/2}$ in Eq. (13). However, according to the scaling considerations in Eq. (13) the last term therein $\sim |t|^{D\nu}$ ($= t^2$

within mean field theory) represents the *leading* non-analytic contribution to the order parameter profile for $t \rightarrow 0$. Therefore one concludes that $P_1^{(3)} = 0$ and the analytic expression in Eq. (A.8) does not capture fully the correct analytic properties of $P_1(\zeta)$. Thus Eq. (A.5) has to be solved numerically.

-
- [1] L. Harnau and S. Dietrich, in *Soft Matter*, edited by G. Gompper and M. Schick (Wiley-VCH, Berlin, 2007), Vol. 3, p. 156.
- [2] J.-P. Hansen and H. Löwen, *Annu. Rev. Phys. Chem.* **51**, 209 (2002).
- [3] V. A. Parsegian, in *Van der Waals forces*, (Cambridge University Press, New York, 2006).
- [4] F. Schlesener, A. Hanke, and S. Dietrich, *J. Stat. Phys.* **110**, 981 (2003).
- [5] L. Harnau and J.-P. Hansen, *J. Chem. Phys.* **116**, 9051 (2002).
- [6] D. Beysens and D. Estève, *Phys. Rev. Lett.* **54**, 2123 (1985).
- [7] V. Gurfein, D. Beysens and F. Perrot, *Phys. Rev. A* **40**, 2543 (1989).
- [8] P. D. Gallagher and J. V. Maher, *Phys. Rev. A* **46**, 2012 (1992).
- [9] P. D. Gallagher, M. L. Kurnaz, and J. V. Maher, *Phys. Rev. A* **46**, 7750 (1992).
- [10] T. Narayanan, A. Kumar, E. S. R. Gopal, D. Beysens, P. Guenoun, and G. Zalczer, *Phys. Rev. E* **48**, 1989 (1993).
- [11] M. L. Kurnaz and J. V. Maher, *Phys. Rev. E* **51**, 5916 (1995).
- [12] M. L. Kurnaz and J. V. Maher, *Phys. Rev. E* **55**, 572 (1997).
- [13] Y. Jayalakshmi and E. W. Kaler, *Phys. Rev. Lett.* **78**, 1379 (1997).
- [14] J.-M. Petit, B. M. Law, and D. Beysens, *J. Colloid Interface Sci.* **202**, 441 (1998).
- [15] B. M. Law, J.-M. Petit, and D. Beysens, *Phys. Rev. E* **57**, 5782 (1998).
- [16] D. Beysens and T. Narayanan, *J. Stat. Phys.* **95**, 5 (1999).
- [17] M. E. Fisher and P. G. de Gennes, *C. R. Acad. Sc. Paris B* **287**, 207 (1978).
- [18] P. G. de Gennes, *C. R. Acad. Ser. II* **292**, 701 (1981).
- [19] B. M. Law, *Prog. Surf. Sci.* **66**, 159 (2001).
- [20] A. Hanke and S. Dietrich, *Phys. Rev. E* **59**, 5081 (1999).
- [21] E. Eisenriegler, *J. Chem. Phys.* **121**, 3299 (2004).
- [22] Z. Dogic and S. Fraden, in *Soft Matter*, edited by G. Gompper and M. Schick (Wiley-VCH, Berlin, 2006), Vol. 2, p. 1.
- [23] E. Eisenriegler, A. Hanke, and S. Dietrich, *Phys. Rev. E* **54**, 1134 (1996).
- [24] R. Guida and J. Zinn-Justin, *J. Phys. A* **31**, 8103 (1998).
- [25] J. L. Cardy in *Phase Transitions and Critical Phenomena*, edited by C. Domb and J. L. Lebowitz (Academic, London, 1986), Vol. 11, p. 55.
- [26] J. L. Cardy, *Phys. Rev. Lett.* **65**, 1443 (1990).
- [27] G. Flöter and S. Dietrich, *Z. Phys. B* **97**, 213 (1995).
- [28] F. David in *Statistical Mechanics of Membranes and Surfaces*, edited by D. Nelson, T. Piran, and S. Weinberg (World Scientific, Singapore, 1989), Vol. 5, p. 158.
- [29] T. W. Burkhardt and E. Eisenriegler, *J. Phys. A: Math. Gen.* **18**, L83 (1985).
- [30] P.-M. König, P. Bryk, K. Mecke, and R. Roth, *Europhys. Lett.* **69**, 832 (2005).
- [31] A. J. Bary and M. A. Moore, *J. Phys. A: Math. Gen.* **10**, 1927 (1977).
- [32] H. W. Diehl and M. Schmock, *Phys. Rev. B* **47**, 5841 (1993).
- [33] K. Binder in *Phase Transitions and Critical Phenomena*, edited by C. Domb and J. L. Lebowitz (Academic, London, 1983), Vol. 8, p. 1.
- [34] H. W. Diehl in *Phase Transitions and Critical Phenomena*, edited by C. Domb and J. L. Lebowitz (Academic, London, 1986), Vol. 10, p. 75.
- [35] T. W. Burkhardt and H. W. Diehl, *Phys. Rev. B* **50**, 3894 (1994).
- [36] M. Abramowitz and I. A. Stegun, *Handbook of Mathematical Functions*, (Dover, New York, 1972).
- [37] E. Eisenriegler, A. Bringer, and R. Maassen, *J. Chem. Phys.* **118**, 8093 (2003).
- [38] E. Eisenriegler, *J. Chem. Phys.* **125**, 204903 (2006).
- [39] J. R. Henderson, in *Fluid Interfacial Phenomena*, edited by C. A. Croxton (Wiley, New York, 1986), p. 555.
- [40] R. Evans, J. R. Henderson, and R. Roth, *J. Chem. Phys.* **121**, 12074 (2004).
- [41] P.-M. König, R. Roth, and K. R. Mecke, *Phys. Rev. Lett.* **93**, 160601 (2004).
- [42] H. Hadwiger, in *Vorlesungen über Inhalt, Oberfläche und Isoperimetrie*, (Springer, Berlin, 1957).
- [43] K. R. Mecke, *Int. J. Mod. Phys. B* **12**, 861 (1998).